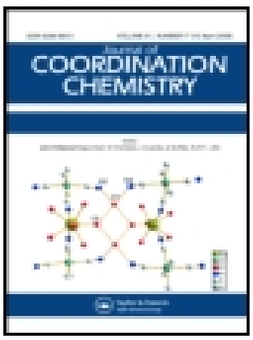

Journal of Coordination Chemistry

ISSN: 0095-8972 (Print) 1029-0389 (Online) Journal homepage: http://www.tandfonline.com/loi/gcoo20

# Synthesis, X-ray characterization and *in vitro* biological approach of dimeric and polymeric mercury(II) complexes with α-keto stabilized sulfur ylide

Seyyed Javad Sabounchei, Mojdeh Sadat Hashemi, Roya Karamian, Seyed Hamed Moazzami Farida, Parviz Gohari Derakhshandeh, Robert W. Gable & Kristof Van Hecke

**To cite this article:** Seyyed Javad Sabounchei, Mojdeh Sadat Hashemi, Roya Karamian, Seyed Hamed Moazzami Farida, Parviz Gohari Derakhshandeh, Robert W. Gable & Kristof Van Hecke (2018): Synthesis, X-ray characterization and *in vitro* biological approach of dimeric and polymeric mercury(II) complexes with α-keto stabilized sulfur ylide, Journal of Coordination Chemistry, DOI: 10.1080/00958972.2018.1510493

**To link to this article:** https://doi.org/10.1080/00958972.2018.1510493

# Synthesis, X-ray characterization and *in vitro* biological approach of dimeric and polymeric mercury(II) complexes with α-keto stabilized sulfur ylide

SEYYED JAVAD SABOUNCHEI*[a], MOJDEH SADAT HASHEMI[a], ROYA KARAMIAN[b], SEYED HAMED MOAZZAMI FARIDA[b], PARVIZ GOHARI DERAKHSHANDEH[c], ROBERT W. GABLE[d] and KRISTOF VAN HECKE*[c]

[a] Faculty of Chemistry, Bu-Ali Sina University, Hamedan, 65174, Iran
[b] Department of Biology, Faculty of Science, Bu-Ali Sina University, P. O. Box 65175/4161, Hamedan, Iran
[c] XStruct, Department of Inorganic and Physical Chemistry, Ghent University, Krijgslaan 281-S3, B-9000 Ghent, Belgium
[d] School of Chemistry, University of Melbourne, Victoria 3010, Australia

Reaction of α-keto stabilized sulfur ylide $(Me)_2SCHC(O)C_6H_4$-*p*-CN (**Y**) with $HgX_2$ (X = Cl, Br and I) led to the formation of new dinuclear products of the type $[HgX_2(Y)]_2$ (X = Cl (**1**), Br (**2**) and I (**3**)). Furthermore, the reaction of the corresponding sulfur ylide (**Y**) with $Hg(NO_3)_2{\cdot}H_2O$ in equimolar ratio, using methanol as a solvent, was shown to produce the polynuclear complex $[(Y)Hg(NO_3)_2]_n$ (**4**). The obtained compounds were characterized using elemental analysis, IR, $^1H$ and $^{13}C$ NMR techniques. The structures of compounds **Y** and **1** were characterized by single-crystal X-ray diffraction analysis. Also, in order to confirm the crystalline nature of complexes **1**-**3**, powder X-ray diffraction (XRD) pattern was used. Likewise, the antioxidant property of the complexes was examined by 1,1-diphenyl-2-picryl-hydrazyl (DPPH) free radical scavenging which revealed the strong-to-moderate radical scavenging ability ($IC_{50}$; 0.163 ± 0.004 to 0.936 ± 0.012 mg·mL$^{-1}$) of the synthesized compounds. Further, results from this study indicated that the compounds possess moderate antibacterial activity.

*Keywords:* Synthesis; Sulfur ylide; Hg(II) Complexes; Single-crystal X-ray diffraction; Antioxidant; Biological activity



## 1. Introduction

Sulfur ylides $R_2S{=}C(R')(R'')$ which are conveniently produced by the treatment of sulfonium salts with base have been recognized as important reagents in organic chemistry [1-6]. Because of high stability and the ambidentate character of α-keto stabilized sulfur ylides, these

*Corresponding authors. Email: jsabounchei@yahoo.co.uk (S.J. Sabounchei); kristof.VanHecke@UGent.be (K. van Heck)

compounds are a suitable choice for organometallic synthesis [7-10]. About 40 years ago, Weleski *et al.* [11] reported a halide-bridged dimeric structure for the Hg(II) halide complexes with sulfur ylides. Soon after, in 1984, Tewari *et al.* [12] managed to report the synthesis of a series of transition metal complexes with various sulfur ylides without further characterization. Sulfur ylides can coordinate to metal ions through the carbanion (C-coordinate) or the enolate (O-coordinate) in three distinct modes: mononuclear (D or E), dinuclear (F) and multinuclear structures (G) (scheme 1) [13-15]. Soft metal ions such as Pd(II), Pt(II), Ag(I), Hg(II), Au(I) and Au(III) coordinate through carbon and this type of coordination is more predominant [16-18]. Whereas O-coordination dominates when the metals involved are hard, *e.g.*, Ti(IV), Zr(IV), and Hf(IV) [19].

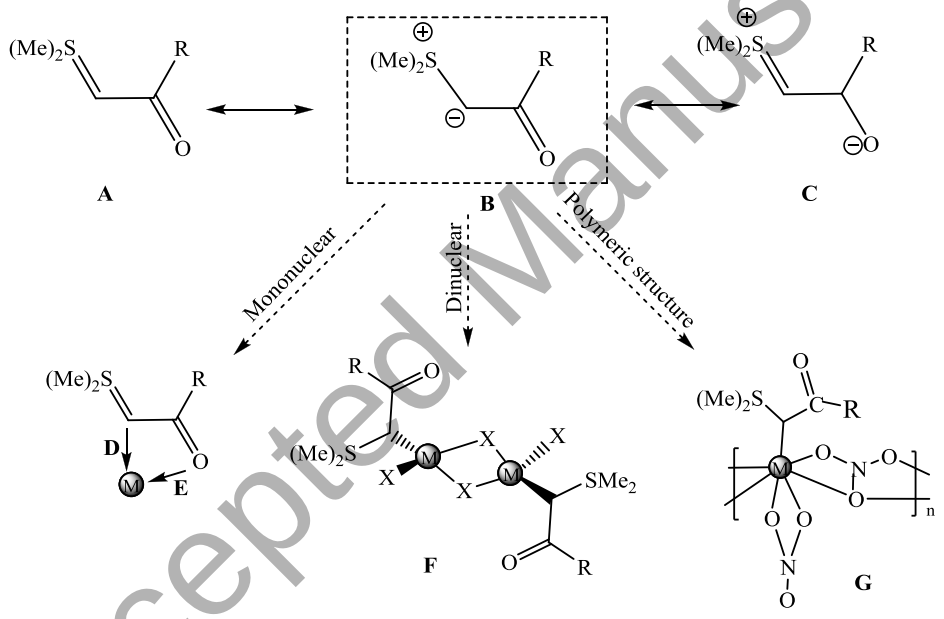


Scheme 1. Canonical binding modes of $(Me)_2SCHC(O)C_6H_4$-*p*-CN to metal ions.

Although a large spectrum of microorganisms coexists in a natural equilibrium with the human body and living environments, uncontrolled fast thriving of microbes can lead to troublesome problems [20, 21]. Therefore, scientists have attempted to develop materials which are capable to prevent the bacterial growth and also to scavenge the free radicals in order to use them in hospital equipment and industrial products such as textile, soap, detergents, household cleaner, health and skin care products. In this context, inorganic materials have received extensive

interest more than organic compounds because of their outstanding advantages such as chemical stability, thermal resistance, safe use and a long active period [22-24]. This paper includes the synthesis, spectroscopic and structural characterization of dinuclear and polymeric complexes of Hg(II) with sulfur ylide. In addition, we assessed *in vitro* antioxidant and antibacterial activities of the synthesized complexes.

## 2. Experimental

### 2.1. *Physical measurements and materials*

All reactions were carried out in the air. All solvents and materials were prepared from commercial sources and were utilized without purification. Melting points were measured with an SMP3 apparatus. IR spectra were recorded on KBr pellets using a Shimadzu 435-U-04 spectrophotometer from 4000-400 $cm^{-1}$. $^{1}H$ and $^{13}C$ NMR spectra were recorded on 250 MHz Bruker and 90 MHz Jeol spectrometers in DMSO-$d_6$ as the solvent at 25 °C. Chemical shifts (δ) are reported relative to internal TMS ($^{1}H$ and $^{13}C$). Coupling constants are given in Hz. Elemental analysis for carbon, nitrogen, hydrogen, and sulfur atoms have been confirmed by utilizing a Perkin Elmer 2400 series analyzer. Powder X-ray diffraction (XRD) patterns were determined with a Philips PW1730 (X-ray diffractometer with Cu as anode material, K-alpha [Å] = 1.54184 and the generator settings 30 mA, 40 KV).

### 2.2. X-*ray crystallography*

Single-crystals of **Y** and **1** were obtained by continuous and gradual evaporation from DMSO. Suitable crystals were selected and mounted on cryoloop and nylonloop with X-ray intensity data collected at 130 K (for **Y**) and 100 K (for **1**) on a Rigaku Oxford Diffraction Supernova Dual Source (Cu at zero) diffractometer equipped with an Atlas CCD detector using ω scans and CuKα (λ = 1.54184 Å) radiation. Interpreted and integrated were the images with the program CrysAlisPro [25]. With the use of Olex2 [26], the structures were solved by direct methods using the ShelXS structure solution program and refined by full-matrix least-squares on $F^2$ using the ShelXL program package [27, 28]. Non-hydrogen atoms were anisotropically refined and the hydrogen atoms in the riding mode and isotropic temperature factors were fixed at 1.2 times U(eq) of the parent atoms (1.5 times for methyl groups).

### 2.3. *Evaluation of biological activities*

**2.3.1. Antioxidant activity.** Antioxidant activities of the complexes were evaluated by DPPH radical scavenging as reported by Mensor *et al*. [29]. Briefly, 2.5 ml of different concentrations of each sample (0.2-1 $mg{\cdot}mL^{-1}$ in DMSO) were added to 1 ml of 0.3 mM DPPH solution and incubated 30 min at room temperature under dark. The reduction of free radicals was measured by reading the absorbance at 517 nm. Ascorbic acid and quercetin were used as reference standards. The antioxidant activity of each sample was calculated from the following formula:

$$\text{DPPH free radical scavenging (\%)} = [1 - (As - Ab)/Ac] \times 100$$

where As is the absorbance of the reaction mixture containing 2.5 mL of sample + 1 mL of DPPH, Ab is the absorbance of the reaction mixture containing 2.5 mL of sample + 1 mL methanol and Ac is the absorbance of the control sample containing 1 mL of DPPH + 2.5 mL methanol. Also, the $IC_{50}$ value, defined as the concentration of the sample leading to 50% reduction of the initial DPPH concentration, was calculated from the linear regression plot of the concentration of the test sample against the mean percentage of the antioxidant activity [30].

**2.3.2. Antibacterial activity.** The synthesized complexes were screened for their antibacterial activities against *Escherichia coli*, *Salmonella typhimurium*, *Klebsiella oxytoca*, and *Shigella dysenteriae* as Gram-negative bacteria and *Listeria monocytogenes*, *Bacillus subtilis*, *Bacillus cereus* and *Staphylococcus aureus* as Gram-positive bacteria. The complexes were dissolved in DMSO to a final concentration of 1 $mg{\cdot}mL^{-1}$ and filtrated using a 0.45 µm Millipore. All complexes were carried using 10 mL of a suspension containing $1.5{\times}10^{8}$ bacteria $mL^{-1}$ and spread on nutrient agar medium. The antibiotics Penicillin, Ampicillin, Vancomycin and Tetracycline were used as positive reference standards, and negative controls were prepared by using DMSO. The inhibition zone diameter and the amount of swelling from the edge of each disc in the plate are given in mm.

**2.3.3. Statistical analysis.** All data obtained from both antioxidant and antibacterial assessments were performed in triplicate. Data were analyzed using a one-way ANOVA and Duncan test and expressed as the mean ± SD. All significance tests were set at $P \leq 0.05$, and the statistics were

analyzed using the SPSS software (IBM Corp. Released 2013. IBM SPSS Statistics for Windows, Version 22.0. Armonk, NY: IBM Corp.). In order to depict the synthesized compounds grouping, cluster analysis (CA) was performed for $IC_{50}$ values of the compounds based on Euclidean similarity index using Unweighted Pair-Group Method with Arithmetic Means (UPGMA) method. Visualization of CA data was performed using PAST software.

### 2.4. *Synthesis*

**2.4.1. Synthesis of [$(Me)_2SCH_2C(O)C_6H_4$-p-CN]Br (S).** 0.11 g (0.5 mmol) of 2-bromo-4′-cyanoacetophenone was dissolved in 15 mL acetone. Then, to the solution was added 0.09 g (1.5 mmol) of dimethyl sulfide. The resulting mixture was allowed to be stirred for 15 h. After the solvent evaporation, being washed with acetone, white sediment was obtained. Yield: 90% (0.13 g); decomposition at 158-162 °C. The product was characterized on the basis of $^1H$, $^{13}C$ NMR and CHNS analysis data that well fitted its structure. *Anal*. Calc. for $C_{11}H_{12}SBrON$ (%): C, 46.16; H, 4.23; S, 11.20. Found: C, 46.32; H, 4.39; S, 11.36. IR (KBr disk), ν ($cm^{-1}$): 1688 (C=O); 831 ($S^+$-$C^-$) and 2234.76 (CN). $^1H$ NMR, DMSO-$d_6$, δ (ppm): 3.02 (s, 6H, $S(CH_3)_2$); 5.64 (s, 2H, $CH_2$); 7.92-8.23 (m, 4H, Ph). $^{13}C$ NMR, DMSO-$d_6$, δ (ppm): 26.64 (s, $S(CH_3)_2$); 54.92 (s, $CH_2$); 115.35 (s, CN); 116.21 (s, Ph); 117.09 (s, Ph); 118.82 (s, Ph); 119.04 (s, Ph); 195.88 (s, CO).

**2.4.2. Synthesis of $(Me)_2SC(H)C(O)C_6H_4$-p-CN (Y).** 0.18 g (0.62 mmol) of **S** was added to 25 mL of NaOH (10%) aqueous solution and then stirred at 25 °C for 15 min. The ylide **Y** was extracted, washed and dried. Yield: 70% (0.09 g); decomposition at 165-166 °C. The product was characterized on the basis of $^1H$, $^{13}C$ NMR, CHNS analysis data that well fitted its structure. *Anal*. Calc. for $C_{11}H_{11}NOS$ (%): C, 64.36; H, 5.40; S, 15.62. Found: C, 64.42; H, 5.46; S, 15.69. IR (KBr disk), ν ($cm^{-1}$): 1572 (C=O), 861.31 ($S^+$-$C^-$) and 2225.61 (CN). $^1H$ NMR, DMSO-$d_6$, δ (ppm): 2.95 (s, 6H, $S(CH_3)_2$); 4.31 (s, 1H, CH); 7.24-7.81 (m, 4H, Ph). $^{13}C$ NMR, DMSO-$d_6$, δ (ppm): 26.75 (s, $S(CH_3)_2$); 53.25 (s, CH); 112.55 (s, CN); 118.94 (s, Ph); 126.42 (s, Ph); 131.80 (s, Ph); 145.01 (s, Ph); 180.33 (s, CO).

**2.4.3. Synthesis of the complexes.** General procedure: 0.2 g (1 mmol) of the sulfur ylide (**Y**) was added to 15 mL of a methanol solution of $HgX_2$ (X = Cl, Br and I) (1 mmol, 5 mL) or

$Hg(NO_3)_2 \cdot H_2O$ (1 mmol, 5 mL) and stirred for 4 h at room temperature. The formed precipitate was filtered, washed with diethyl ether and dried.

*2.4.3.1. Data for [(Y)$HgCl_2$]$_2$ (**1**).* Yield 0.2 g, 92%. *Anal*. Calc. for $C_{22}H_{22}Cl_4Hg_2N_2O_2S_2$ (%): C, 27.71; H, 2.33; S, 6.73; N, 2.94. Found: C, 27.80; H, 2.42; S, 6.80; N, 3.03. Decomposition at 208-210 ºC. IR (KBr disk), $\nu$(cm$^{-1}$): 1655 (CO); 856 ($C^-$-$S^+$) and 2237 (CN). $^1$H NMR, DMSO-$d_6$, δ (ppm): 2.91 (s, 6H, $S(CH_3)_2$); 5.49 (s, 1H, CH); 7.91-8.11 (m, 4H, Ph). $^{13}$C NMR, DMSO-$d_6$, δ (ppm): 27.12 (s, $S(CH_3)_2$); 64.58 (s, CH); 115.22 (s, CN); 118.60 (s, Ph); 128.63 (s, Ph); 132.93 (s, Ph); 139.13 (s, Ph); 190.56 (s, CO).

*2.4.3.2. Data for [(Y). $HgBr_2$]$_2$ (**2**).* Yield 0.2 g, 89%. *Anal*. Calc. for $C_{22}H_{22}Br_4Hg_2N_2O_2S_2$ (%): C, 23.36; H, 1.96; S, 5.67; N, 2.48. Found: C, 23.54; H, 2.14; S, 5.85; N, 2.66. Decomposition at 200-202 ºC. IR (KBr disk): $\nu$(cm$^{-1}$) 1653 (CO); 745 ($C^-$-$S^+$) and 2237 (CN). $^1$H NMR, DMSO-$d_6$, δ (ppm): 2.89 (s, 6H, $S(CH_3)_2$); 5.43 (s, 1H, CH); 7.92-8.11 (m, 4H, Ph). $^{13}$C NMR, DMSO-$d_6$, δ (ppm): 27.21 (s, $S(CH_3)_2$); 64.52 (s, CH); 114.98 (s, CN); 118.67 (s, Ph); 128.60 (s, Ph); 132.90 (s, Ph); 139.69 (s, Ph); 189.58 (s, CO).

*2.4.3.3. Data for [(Y).$HgI_2$]$_2$ (**3**).* Yield 0.2 g, 87%. *Anal*. Calc. for $C_{22}H_{22}I_4Hg_2N_2O_2S_2$ (%): C, 20.03; H, 1.68; S, 4.86; N, 2.12. Found: C, 20.21; H, 1.82; S, 5.04; N, 2.3. Decomposition at 186-188 °C. IR (KBr disk), $\nu$(cm$^{-1}$): 1640 (CO); 825 ($C^-$-$S^+$) and 2234 (CN). $^1$H NMR, DMSO-$d_6$, δ (ppm): 2.90 (s, 6H, $S(CH_3)_2$); 5.32 (s, 1H, CH); 7.74-8.12 (m, 4H, Ph). $^{13}$C NMR, DMSO-$d_6$, δ (ppm): 27.35 (s, $S(CH_3)_2$); 64.22 (s, CH); 114.65 (s, CN); 118.57 (s, Ph); 128.57 (s, Ph); 132.85 (s, Ph); 140.37 (s, Ph); 188.35 (s, CO).

*2.4.3.4. Data for [(Y). $Hg(NO_3)_2$]$_n$ (**4**).* Yield 0.2 g, 91%. *Anal*. Calc. for $C_{11}H_{11}O_7N_3SHg$ (%): C, 24.93; H, 2.09; S, 6.05; N, 7.93. Found: C, 25.09; H, 2.27; S, 6.23; N, 8.11. Decomposition at 193-195 °C. IR (KBr disk), $\nu$(cm$^{-1}$): 1661 (CO); 1384 (NO); 858 ($C^-$-$S^+$) and 2234 (CN). $^1$H NMR, DMSO-$d_6$, δ (ppm): 2.71, 2.98 (s, 6H, $S(CH_3)_2$); 5.51- 5.97 (d, 1H, CH); 7.61-8.33 (m, 4H, Ph). $^{13}$C NMR, DMSO-$d_6$, δ (ppm): 26.95 (s, $S(CH_3)_2$); 60.36, 67.55 (s, CH); 115.23 (s, CN); 114.10 (s, Ph); 121.18 (s, Ph); 121.65 (s, Ph); 130.86 (s, Ph); 135.8 (s, Ph); 160.15 (s, Ph); 192.10, 194.57 (s, CO).

## 3. Results and discussion

### 3.1. *Synthesis*

Reaction of dimethyl sulfide with the 2-bromo-4′-cyanoacetophenone in equimolar ratio gave the compound **S**. The resulted **S** was treated with NaOH 10% to obtain the sulfur ylide. The reaction of sulfonium salt with $HgX_2$ (X = Cl, Brand I) and $Hg(NO_3)_2{\cdot}H_2O$ in [1:1] ratio yielded the dimeric and polymeric complexes, **1**-**3** and **4** (scheme 2). X-ray quality crystals of compounds **Y** and **1** were grown by slow evaporation from DMSO over 3 weeks. Because of the very low solubility of these complexes in most common solvents such as chloroform, acetone, and ethanol, DMSO was found to be a suitable solvent for the NMR spectroscopy and crystallization.

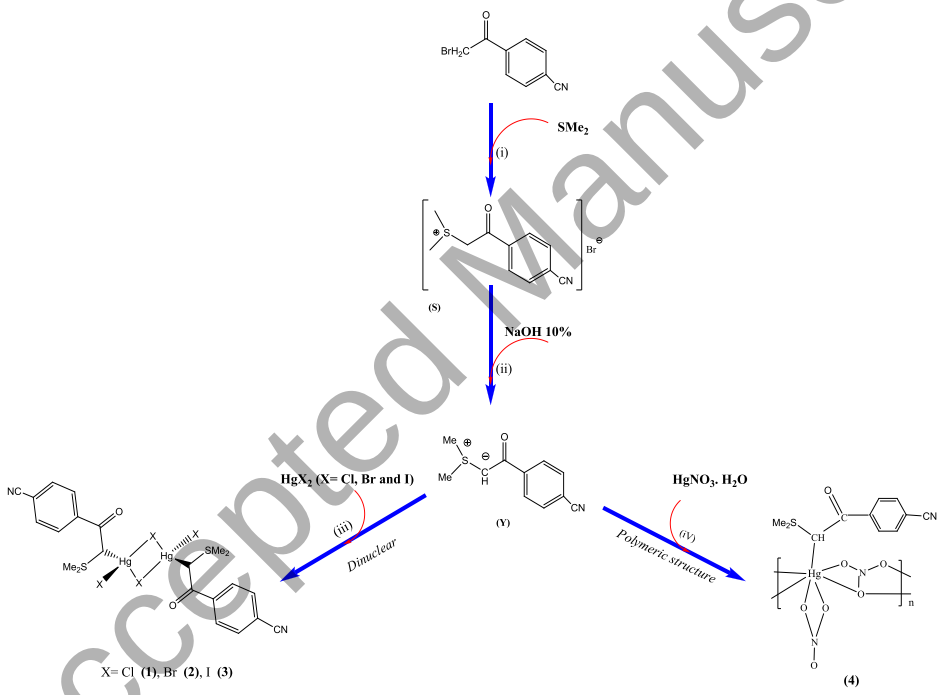


Scheme 2. (i); acetone for 15 h, (ii); 30 min, (iii) and (iv); methanol for 4 h.

### 3.2. *Spectroscopy*

All structures were characterized by $^{1}H$ and $^{13}C$ NMR spectroscopy and other conventional techniques such as IR and elemental analysis. The CHNS elemental analysis of the mercury complexes **1**-**4** shows a 1:1 stoichiometry between the sulfur ylide and $HgX_2$ (X = Cl, Br, I or $NO_3$). Table 1 summarizes the spectroscopic data for synthesis of compounds.

The ν(CO) in the IR spectrum of the sulfonium salt is observed as a sharp band at 1688 $cm^{-1}$, showing a higher frequency shift than the related sulfur ylide (1579 $cm^{-1}$). This absorption band, that is very sensitive to variations in bond order, is observed for complexes **1-4** at higher frequencies (1640-1661 $cm^{-1}$) compared to the sulfur ylide. Also, the infrared spectrum of complex **4** is a good indicator for detection of polymerization. The $NO_2$ group in the infrared spectrum has two strong peaks at 1300-1390 and 1530-1600 $cm^{-1}$. These peaks were assigned to the symmetric and asymmetric stretching vibrations of the $NO_2$ group in the $Hg(NO_3)_2{\cdot}H_2O$, respectively. The peak of the asymmetric stretching vibration has been removed and the peak at 1384 $cm^{-1}$ is related to the vibration of N-O stretching in complex **4** [31].

The $^1H$ NMR spectrum of the sulfur ylide exhibits methinic proton signals at lower frequencies in contrast to that of the sulfonium salt. This upfield shift is due to the vicinity of a formal negative charge on the methinic carbon, which increase the electron density in C-H bond. The chemical shifts of the methinic protons of complexes can be used to determine the coordination mode of the ligands to the metal center. The $^1H$ NMR signals for SCH group of all complexes, due to removal of some electron density in S-C bonds, occur at higher frequencies in comparison to those of the sulfur ylide [32]. Based on our results, the coordination of the sulfur ylide to metal ions occurs through the ylidic carbon atom.

The most interesting aspect of the $^{13}C$ NMR spectra of the complexes, due to the change in hybridization of the ylidic carbon atom from $sp^2$ to $sp^3$, is the lower shielding of the ylidic carbon atoms. The $^{13}C$ chemical shifts of the CO group in all complexes were found to be around 190 ppm, relative to 180 ppm noted for the same carbon in the parent ylides, indicating a decreased shielding of this carbon atom in mercury complexes. No coupling to ($^{199}Hg$, 16.8% abundance, I = 1/2) was observed at room temperature in $^1H$ and $^{13}C$ NMR spectra [12].

### 3.3. *Crystal structure analysis*

X-ray quality crystals of the ligand **Y** and complex **1** were grown by the slow evaporation from DMSO over 3 weeks. The molecular structures of **Y** and **1** were determined by single-crystal X-ray diffraction analysis. The molecular structure of these compounds is shown in figures 1 and 2, respectively. Summarized in table 2 are crystallographic data concerning data collection and structure solution and refinement. Selected bond lengths and angles are presented in tables S1 and S2 of Supporting Information. Compound **Y** was crystallized in the

centrosymmetric monoclinic space group P21/c. In the structure of **Y**, the S1-C1 bond length of 1.7127(12) Å is significantly less than that of the two S-C single bonds (S1-C10 = 1.8002(13) Å and S1-C11 = 1.7993(12) Å). The dihedral angle between the aromatic ring and the keto group is 15.80(6)°. Weak C-H… N and C-H… O interactions link the molecules into a 2D polymer lying in the plane. Compound **1** is crystallized in the centrosymmetric triclinic space group P-1. The asymmetric unit consists of one **Y** ligand, one Hg(II) ion and two $Cl^-$ ions. A dinuclear structure is built up around an inversion center, similar to previously reported C-coordinated Hg(II) halide complexes of dimethyl sulfur ylides [12, 13, 16]. Each Hg(II) center is four-coordinate and shows an $sp^3$ hybridization, with its coordination environment, including a short terminal Hg-Cl bond (2.386(2) Å), one Hg-C bond (2.164(7) Å), and two asymmetric bridging Hg-Cl bonds (2.6915(15) and 2.7537(15) Å). When compared to analogous C-coordinated dinuclear Hg(II) chloride complexes of triphenyl phosphonium ylides, the Hg-C bond distances are significantly shorter in the sulfur ylides than the equivalent distances in the phosphonium analogs, pointing towards a higher basicity of the sulfur ylides, as previously explained [12, 13]. The six angles subtended by the different ligands at the Hg(II) center vary from 84.39(5)° to 142.35(16)°, indicating a highly distorted tetrahedral coordination environment. The two Hg(II) atoms and two bridging chlorides are perfectly coplanar, while the internuclear distance between the two Hg(II) atoms is 4.0344(5) Å. Comparable features have been previously reported for similar dimethyl sulfur ylides [12, 13, 16]. In the crystal packing, short π-π ring interactions are observed between the cyanophenyl rings (centroid-centroid distances of 3.921(4) Å and 3.910(4) Å).

### 3.4. *Evaluation of biological activities*

**3.4.1. Antioxidant activity.** DPPH has been broadly used to test the antioxidant potential of different compounds. The antioxidants have the ability to reduce stable radicals changing the characteristic deep purple color ($\lambda_{max}$ = 515-517 nm) of DPPH to the yellow-colored nonradical diphenyl-picrylhydrazine (DPPH-H) [33, 34]. Results of DPPH assay are summarized in table 3 (see also table S3 in Supporting Information). According to our results, most of the synthesized compounds display tremendous dose-dependent (0.2-1 $mg{\cdot}mL^{-1}$) antiradical activity (46.81-70.53%) (table 3). The scavenging activity is higher when the $IC_{50}$ value is low. The effectiveness of the samples as DPPH radical scavengers ranged in the following descending

order: (i) ylide ($IC_{50}$ = 0.16±0.01 mg·mL$^{-1}$) < (ii) $[HgCl_2(Y)]_2$ ($IC_{50}$ = 0.19±0.05 mg·mL$^{-1}$) < (iii) $[HgI_2(Y)]_2$ ($IC_{50}$ = 0.52±0.01 mg·mL$^{-1}$) < (iv) $[HgBr_2(Y)]_2$ ($IC_{50}$ = 0.53±0.01 mg·mL$^{-1}$) < (v) $[Hg(NO_3)_2(Y)]_n$ complexes ($IC_{50}$ = 0.94±0.01 mg·mL$^{-1}$). Results showed that (i) and (ii) were compared with ascorbic acid and quercetin as standard antioxidant in radical scavenging. A comparison between the DPPH radical scavenging activity of the synthesized compounds and some of other ylide-based compounds studied in the literature is shown in table 4. The results exhibited that **1** was nearly twice as active in DPPH radical scavenging abilities as those of $C^3$, being the strongest antioxidant complex studied by our group [35]. In addition to **1**, the other studied complexes in this work had higher antioxidant properties than those previously reported [35]. Altogether, the compounds with sulfur ylides and their Hg(II) complexes can significantly improve the radical scavenging activity in comparison to phosphorus ylides and their Pd(II) complexes. Based on the $IC_{50}$ values, the studied compounds could be divided into three distinct parts (figure 3). The first part which consisted of quercetin, ascorbic acid, and **Y** showed low $IC_{50}$ values (0.13-0.16 mg·mL$^{-1}$). It could be pointed out that these compounds possess the high antioxidant potential. The second part was made of **1**, **2** and **3**. This group which has dimeric structure of mercury(II) halides was characterized by a moderate amount of $IC_{50}$. The $IC_{50}$ values of this compound varied from 0.19 to 0.53 mg·mL$^{-1}$. The third part constituted of complex **4** and showed high $IC_{50}$ values (0.94 mg·mL$^{-1}$) (figure 3). This compound has polymeric structure of mercury(II) nitrate.

**3.4.2. Antibacterial activity.** Results showed that both Gram-negative and -positive bacteria were annihilated by the complexes (table 5). However, the complexes represented antibacterial activity against the Gram-negative bacteria more than -positive ones, which can be attributed to the differences in their cell wall structures in that the cell wall of Gram-positive bacteria is made of a thick layer of peptidoglycan, comprising of linear polysaccharide chains cross-linked by short peptides thus forming more rigid structure leading to the difficult penetration of the compounds while in the Gram-negative bacteria, the cell wall possesses only a thinner layer of peptidoglycan [33].

According to our results, the Hg(II)-ligand (average inhibition zone: 32 mm) and the $HgNO_3$ complex (average inhibition zone: 27 mm) represented a significant effect on Gram-negative and -positive bacteria, respectively. Apparently, *Escherichia coli* (-) and *Klebsiella*

*oxytoca*(-) were the most sensitive bacteria and conversely, *Listeria monocytogenes* (+) was one of the most resistant synthesized compounds. In a comparison of their antibacterial activities with those of reference antibiotics, the complexes seem to have extraordinary inhibitory potency against the bacteria tested. As can be seen in table 6, the antibacterial activity of Hg(II) complex with sulfur ylide showed the significant effect against Gram-positive bacteria, especially *B. cereus* and *S. aureus*, in comparison to the other metal complexes with different ylide ligands. Generally, the antibacterial activity of a compound is ascribed mainly to its major components. On the other hand, our findings suggest that the synthesized Hg(II) complexes can be considered as potential biocides in composite materials.

### 3.5. *Powder XRD studies*

The XRD pattern of **1-3** was considered in a domain of 10 to 80 degrees. This pattern indicates the crystalline nature for the complexes. Peak width (FWHM) was investigated. The prominent peaks of the diffraction pattern were indexed (graph 1). The obtained data are collected in table 7. The crystallite size D of the complexes was calculated using the Debye-Sherrer formula $D = K\lambda/(ß\text{Cos}\theta)$, with λ being the X-ray wavelength (λ = 0.154 nm), K is the Scherrer constant (0.9), *ß* the peak width of half-maximum (FWHM) and $\theta$ is the Bragg diffraction angle. The interplanar distance was calculated via the Bragg equation: $dhkl = \lambda/(2\sin\theta)$, (λ : Cu radiation (0.154184 nm).

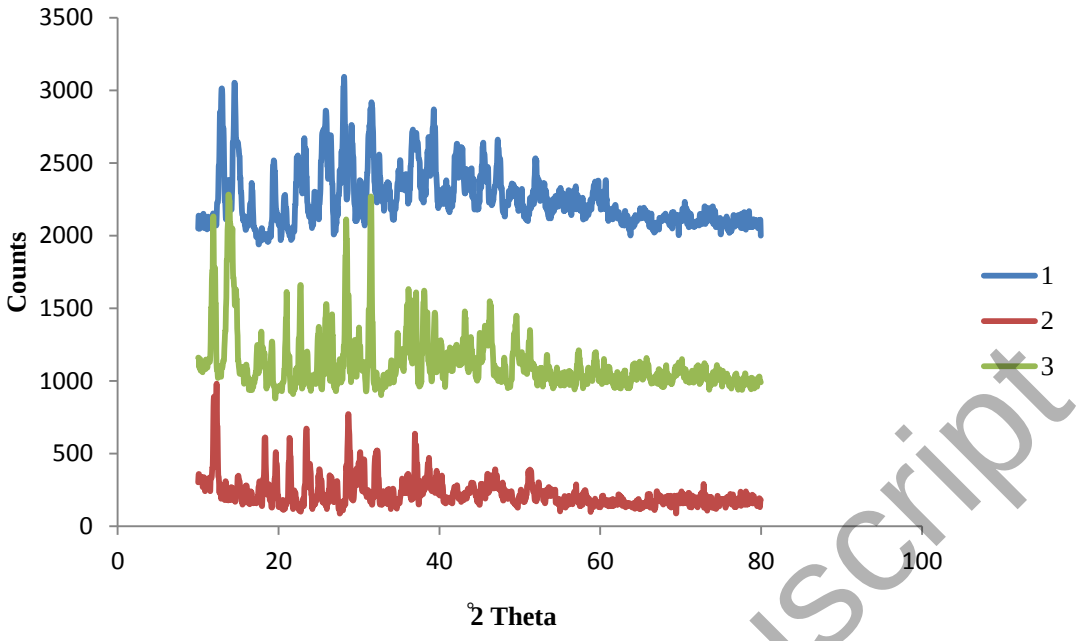


Graph 1. XRD graph of complexes **1**-**3**.



## 4. Conclusion

This study portrays the synthesis and characterization of dimeric and polymeric Hg(II) complexes of sulfur ylide. The structure of the compounds was determined successfully by IR, $^{1}H$, $^{13}C$ NMR spectroscopic techniques and elemental analysis. Based on the physicochemical and spectroscopic data, we propose a monodentate C-coordinate of the sulfur ylide to the metal, which is further confirmed by the X-ray crystal structure of **1**. In this complex, the related ligand is coordinated to one mercury atom through the ylidic carbon atom. In the following, a symmetric halide-bridged dimeric structure to the Hg(II) chloride is formed. Furthermore, our results revealed the antioxidant potency and antibacterial activity of the complexes on the growth of both Gram-positive and -negative bacteria. The XRD pattern indicated crystalline nature for **1-3**.

## Supplementary material

CCDC 1559666-1572297 contain the supplementary crystallographic data for **Y** and **1**. These data can be obtained free of charge via www.ccdc.cam.ac.uk/conts/retrieving.html (or from the Cambridge Crystallographic Data Centre, 12 Union Road, Cambridge CB2 1EZ, UK; Fax: +44-1223-336033; or E-mail: deposit@ccdc.cam.ac.uk).

**Acknowledgements**

We are grateful to Bu-Ali Sina University for financial support. KVH thanks the Hercules Foundation (project AUGE/11/029 "3D-SPACE: 3D Structural Platform Aiming for Chemical Excellence") for funding and the Research Foundation - Flanders (FWO) (project 1.5.216.15N) for financial support.

**References**

[1] D. Janardanan, R.B. Sunoj. *J. Org. Chem.*, **72**, 331 (2007).

[2] D. Meng, P. Bertinato, A. Balog, T. Kamenecka, E. Sorenson, S. Danishefsky. *J. Am. Chem. Soc.*, **119**, 10073 (1997).

[3] J.S. Lai, R.F. Wu, I.J.B. Lin. *J. Organomet. Chem.*, **393**, 431 (1990).

[4] I.J.B. Lin, H.C. Shy, C.W. Liu, L.K. Liu, S.K. Yeh. *J. Chem. Soc., Dalton Trans.*, 2509 (1990).

[5] R.F. Wu, I.J.B. Lin, G.H. Lee, M.C. Cheng, Y. Wang. *Organometallics*, **9**, 126 (1990).

[6] P. Leoni, F. Marchetti, M. Paoletti. *Organometallics*, **16**, 2143 (1997).

[7] J.S. Clark, Nitrogen, Oxygen and Sulfur Ylide Chemistry, A Practical Approach in Chemistry. Oxford University Press, Britain (2002).

[8] V.K. Aggarwal, J.-L. Vasse. *Org. Lett.*, **5**, 3987 (2003).

[9] S. Deuerlein, D. Leusser, U. Flierler, H. Ott, D. Stalke. *Organometallics*, **27**, 2306 (2008).

[10] M. Gandelman, K.M. Naing, B. Rybtchinski, E. Poverenov, Y. Ben-David, N. Ashkenazi, R.M. Gauvin, D. Milstein. *J. Am. Chem. Soc.*, **127**, 15265 (2005).

[11] E.T. Weleski Jr, J.L. Silver, M.D. Jansson, J.L. Burmeister. *J. Organomet. Chem.*, **102**, 365 (1975).

[12] R.S. Tewari, A.K. Awasthi. *J. Organomet. Chem.*, **271**, 403 (1984).

[13] J.A. Teagle, J.L. Burmeister. *Inorg. Chim.Acta*, **118**, 65 (1986).

[14] S.J. Sabounchei, F.A.Bagherjeri, C. Boskovic, R.W. Gable, R. Karamian, M. Asadbegy. *Polyhedron*, **53**, 1 (2013).

[15] S.J. Sabounchei, F. Akhlaghi Bagherjeri, C. Boskovic, R.W. Gable. *J. Mol. Struct.*, **1046**, 39 (2013).

[16] M. Kalyanasundari, K. Panchanatheswaran, W.T. Robinson. H. Wen. *J. Organomet. Chem.*, **491**, 103 (1995).

[17] (a) R. Usón, J. Forniés, R. Navarro, P. Espinet, C. Mendívil. *J. Organomet. Chem*., **290**,125 (1985). (b) J. Vicente, M.T. Chicote, I. Saura-Llamas, J. Turpin, J. Fernandez-Baeza. *J.Organomet. Chem*., **333**, 129 (1987). (c) J. Vicente, M.T. Chicote, J. Fernandez-Baeza, J. Martin, I. Saura-Llamas, J. Turpin, P.G. Jones. *J. Organomet. Chem*., **331**, 409 (1987). (d) H. Koezuka, G. Matsubayashi, T. Tanaka. *Inorg. Chem*., **15**, 417 (1976).

[18] S.J. Sabounchei, A. Hashemi, A. Sedghi, M. Bayat, F. AkhlaghiBagherjeri, R.W. Gable. *J. Mol. Struct.*, **1135**, 174 (2017).

[19] J.A. Albanese, D.L. Staley, A.L. Rheingold, J.L. Burmeister. *Inorg. Chem.*, **29**, 2209 (1990).

[20] C.K. Bower, J.E. Parker, A.Z.Higgins, M.E.Oest, J.T.Wilson, B.A.Valentine, M.K. Bothwell, J. McGuire. *Colloids Surf., B*, **25**, 81 (2002).

[21] L. Baikun, B.E. Logan. *Colloids Surf., B*, **36**, 81 (2004).

[22] R. Dastjerdi, M. Montazer. *Colloids Surf., B*, **79**, 5 (2010).

[23] J.J. Hwang, T.W. Ma. *Mater. Chem. Phys.*, **136**, 613 (2012).

[24] L. Bowen, Y. Shuhui, J.Y. Hwang, S. Shangzhao. *J. Miner. Mater. Charactd. Eng.*, 1 (2002).

[25] O.D. Rigaku, CrysAlis PRO, Rigaku Oxford Diffraction, Yarnton, England (2015).

[26] O.V. Dolomanov, L.J. Bourhis, R.J. Gildea, J.A.K. Howard, H. Puschmann. *J. Appl. Cryst.*, **42**, 339 (2009).

[27] G.M. Sheldrick. *J. Appl. Crystallogr.*, **A 71**, 3 (2015).

[28] G.M. Sheldrick. *Acta Crystallogr.*, **C 71**, 3 (2015).

[29] L.L. Mensor, F.S. Menezes, G.G. Leitão, A.S. Reis, T.C.D. Santos, C.S. Coube, S.G. Leitão. *Phytother. Res.*, **15**, 127 (2001).

[30] A.B. Ribeiro, V.D.S. Bolzani, M. Yoshida, L.S. Santos, M.N. Eberlin, D.H. Silva. *J. Braz. Chem. Soc.*, **16**, 526 (2005).

[31] S.J. Sabounchei, H. Nemattalab, H.R. Khavasi. *J. Organomet. Chem.*, **692**, 5440 (2007).

[32] S.J. Sabounchei, F.A. Bagherjeri, Z. Mozafari, C. Boskovic, R.W. Gable, R. Karamian, M. Asadbegy. *Dalton Trans.*, **42**, 2520 (2013).

[33] T.A. Ibrahim, H.M. El-Hefnawy, A.A. El-Hela. *Nat. Prod. Res.*, **24**, 1537 (2010).

[34] C. Kontogiorgis, D. Hadjipavlou-Litina. *J. Enzyme Inhib. Med. Chem.*, **18**, 63 (2003).

[35] S.J. Sabounchei, M. Ahmadi, Z. Nasri, E. Shams, S. Salehzadeh, Y. Gholiee, R. Karamian, M. Asadbegy, S. Samiee. *CR Chim.*, **16**, 159 (2013).

[36] S.J. Sabounchei, M. Ahmadianpoor, A. Hashemi, F. Mohsenzadeh, R.W. Gable. *Inorg. Chim. Acta*, **458**, 77 (2017).

[37] S.J. Sabounchei, F. Akhlaghi Bagherjeri, C. Boskovic, R.W. Gable, R. Karamian, M. Asadbegy. *Polyhedron*, **53**, 1 (2013).

[38] S.J. Sabounchei, M. Panahimehr, M. Hossinzadeh, R. Karamian, M. Asadbegy, A. Masumi. *J. Mol. Struct.*, **1061**, 90 (2014).

[39] S.J. Sabounchei, M. Pourshahbaz, A. Hashemi, M. Ahmadi, R. Karamian, M. Asadbegy, H.R. Khavasi. *J. Organomet. Chem.*, **761**, 111 (2014).

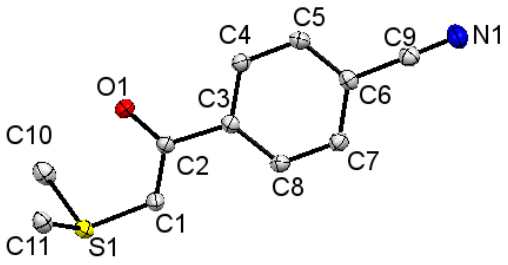


Figure 1. ORTEP view of the X-ray crystal structure of **Y** with atom labeling scheme. H atoms are omitted for clarity.

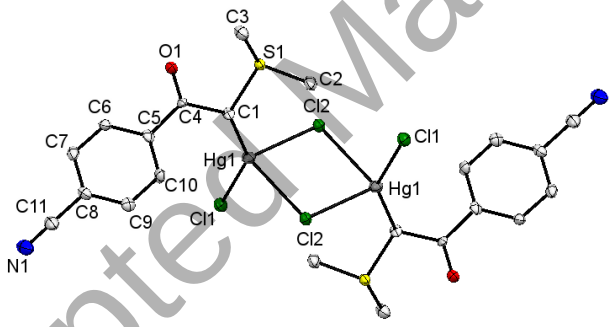


Figure 2. ORTEP view of the X-ray crystal structure of **1**, with atom labeling scheme. H atoms are omitted for clarity.

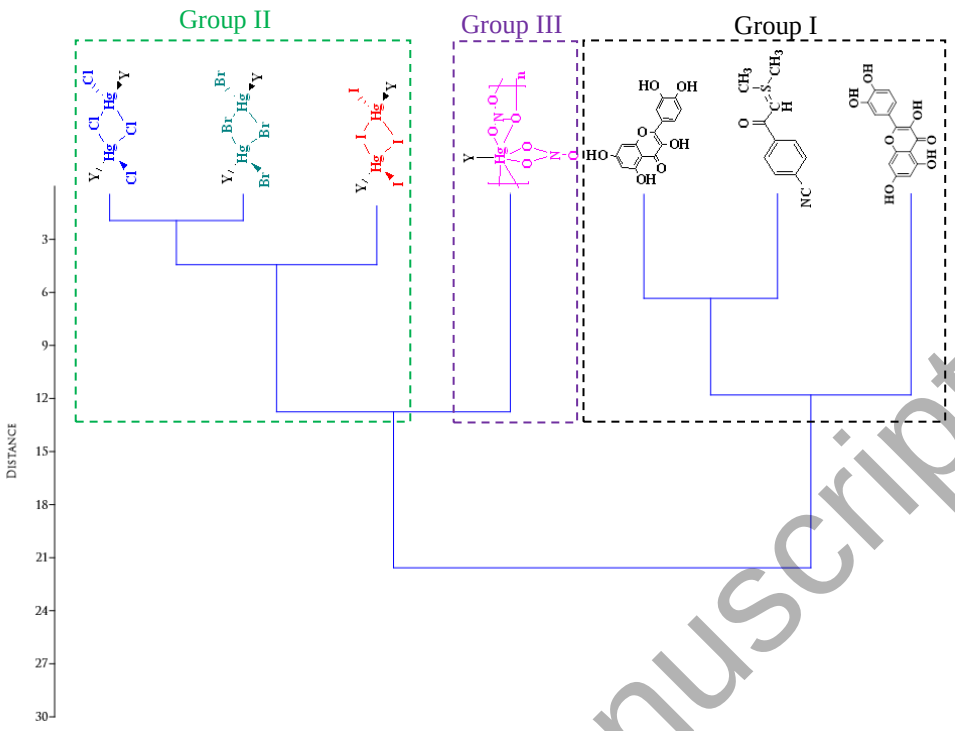


Figure 3. Dendrogram obtained from the cluster analysis of the synthesized compounds and antioxidant standards based on the antioxidant activity ($IC_{50}$ value).

Table 1. Spectroscopic data for compounds **S**, **Y** and **1**-**4**.

| Compound | IR; ν(CO) $cm^{-1}$ | $^{1}H$ NMR; δ(SCH) ppm | $^{13}C$ NMR; δ(SCH) ppm | $^{13}C$ NMR; δ(CO) ppm |
|---|---|---|---|---|
| S | 1688 | 5.64 | 54.92 | 195.88 |
| Y | 1579 | 4.31 | 53.25 | 180.33 |
| 1 | 1655 | 5.49 | 64.58 | 190.56 |
| 2 | 1653 | 5.43 | 64.52 | 189.58 |
| 3 | 1640 | 5.32 | 64.23 | 188.39 |
| 4 | 1661 | 5.51 and 5.97 | 60.36 and 67.55 | 192.10 and 194.57 |

Table 2. Crystallographic data for **Y** and **1**.

| | **Y** | **1** |
|---|---|---|
| Empirical formula | $C_{11}H_{11}NOS$ | $C_{22}H_{22}Cl_4Hg_2N_2O_2S_2$ |
| Formula weight/gmol$^{-1}$ | 205.27 | 953.52 |
| T/K | 130.01 (10) | 100.0 (1) |
| Radiation/Å | CuKα (λ = 1.54184) | CuKα (λ = 1.54184) |
| Crystal system | Monoclinic | Triclinic |
| Space group | $P2_1/c$ | P-1 |
| a/Å | 5.38363(11) | 6.9757(6) |
| b/Å | 8.15920(18) | 7.7187(5) |
| c/Å | 22.8755(5) | 14.0471(10) |
| α/° | 90 | 77.598(6) |
| β/° | 91.4503(19) | 87.630(7) |
| γ/° | 90 | 66.785(7) |
| Volume/Å $^3$ | 1004.51(4) | 678.09(10) |
| Z | 4 | 1 |
| ρcalc /gcm$^{-3}$ | 1.357 | 2.335 |
| μ/mm$^{-1}$ | 2.566 | 25.284 |
| F (000) | 432.0 | 444.0 |
| Crystal size/mm$^3$ | 0.337 × 0.252 × 0.056 | 0.127 × 0.056 × 0.044 |
| 2Θ range for data collection/° | 7.732 to 153.746 | 6.45 to 150.404 |
| Index ranges | $-6 \le h \le 5$, $-10 \le k \le 10$, $-28 \le l \le 28$ | $-8 \le h \le 8$, $-9 \le k \le 9$, $-17 \le l \le 17$ |
| Reflections collected | 8244 | 12920 |
| Independent reflections | 2110 [Rint = 0.0202, R sigma = 0.0170] | 2752 [Rint = 0.0693, R sigma = 0.0435] |
| Data / restraints / parameters | 2110 / 0 / 129 | 2752 / 0 / 156 |
| Final R indices [Io > 2σ (Io)] | R1 = 0.0296, wR2 = 0.0821 | R1 = 0.0396, wR2 = 0.0987 |
| Final R indexes [all data] | R1 = 0.0303, wR2 = 0.0832 | R1 = 0.0432, wR2 = 0.1013 |
| Largest diff. peak/hole /e Å$^{-3}$ | 0.30/-0.33 | 1.32/-1.53 |
| Goodness-of-fit on $F^2$ | 1.042 | 1.062 |

Table 3. Scavenging activity (%) and $IC_{50}$ value of $[HgX_2(Y)]_2$ (**Y**: $(Me)_2SC(H)C(O)C_6H_4$-*p*-CN, X: Cl (**1**), Br (**2**), I (**3**), $NO_3$ (**4**)) at different concentrations ($mg{\cdot}mL^{-1}$), quercetin and ascorbic acid as antioxidant standards.

| Sample | Concentration ($mg{\cdot}mL^{-1}$) | | | | | Average | $IC_{50}$ Value ($mg{\cdot}mL^{-1}$) |
|---|---|---|---|---|---|---|---|
| | 0.2 | 0.4 | 0.6 | 0.8 | 1 | | |
| **Y** | 61.20±1.65[b] | 65.47±0.70[b] | 70.83±1.15[b] | 75.04±1.37[b] | 80.12±0.54[a] | 70.53 | 0.16±0.01[c] |
| **1** | 53.50±0.73[c] | 48.26±0.14[e] | 64.80±1.15[c] | 68.33±0.64[c] | 71.40±0.73[b] | 61.25 | 0.19±0.05[c] |
| **2** | 54.73±1.01[c] | 57.80±0.79[d] | 56.38±0.76[e] | 56.57±0.25[e] | 57.28±0.25[c] | 56.56 | 0.52±0.01[b] |
| **3** | 61.01±1.22[b] | 60.82±0.45[c] | 57.60±0.59[d] | 60.39±0.88[d] | 59.27±0.36[c] | 59.81 | 0.53±0.01[b] |
| **4** | 45.79±0.65[d] | 45.89±0.31[f] | 43.06±0.63[f] | 46.44±0.57[f] | 53.40±0.49[d] | 46.92 | 0.94±0.01[a] |
| Ascorbic acid | 71.47±1.00[a] | 73.75±0.99[a] | 77.07±1.51[a] | 78.86±1.53[a] | 80.89±1.09[a] | 76.41 | 0.14±0.01[c] |
| Quercetin | 76.11±0.69[a] | 81.13±1.01[a] | 86.85±1.81[a] | 88.13±0.92[a] | 91.85±1.32[a] | 84.81 | 0.13±0.01[c] |

[a] Experiment was performed in triplicate and expressed as mean ± SD. Values along each column with different superscripts are significantly different ($P< 0.05$).

Table 4. Comparison of DPPH radical scavenging activity (%) of the studied compounds with the other ylide derivates as reported in literature.

| Compound | Average percentage of scavenging activity (%) | Reference |
|---|---|---|
| **1** | 61.25 | This work |
| **2** | 56.56 | This work |
| **3** | 59.81 | This work |
| **4** | 46.92 | This work |
| $C^1$ | 30.55 | [35] |
| $C^2$ | 32.86 | [35] |
| $C^3$ | 35.53 | [35] |
| $C^4$ | 31.67 | [35] |

*Note*: [(dppe)Pd($Ph_2PCH_2PPh_2C(H)C(O)PhX$)] $(OSO_2CF_3)_2$ (X = Br ($C^1$), Cl ($C^2$), $NO_2$($C^3$), $OCH_3$($C^4$))

Table 5. Antibacterial activity of $[HgX_2(Y)]_2$ (**Y**: $(Me)_2SC(H)C(O)C_6H_4$-*p*-CN, X: Cl (**1**), Br (**2**), I (**3**), $NO_3$ (**4**)), antibiotics (positive controls) and DMSO (negative control) against the studied bacterial strains.

| Sample | Inhibition zone (mm) | | | | | | | |
|---|---|---|---|---|---|---|---|---|
| | *E.coli* | *S. typhimurium* | *K. oxytoca* | *S. dysenteriae* | *L. monocytogenes* | *B. subtilis* | *B. cereus* | *S. aureus* |
| **Y** | 15±0.43 | 20±0.18 | 20±0.78 | 29±0.35 | 44±0.65 | 30±0.26 | 14±0.24 | 38±0.96 |
| **1** | 13±0.56 | 28±0.59 | 15±0.84 | 18±0.29 | 20±0.17 | 15±0.29 | 25±0.12 | 26±0.24 |
| **2** | 17±0.51 | 30±0.63 | 21±0.18 | 12±0.17 | 31±0.35 | 20±0.73 | 30±0.27 | 14±0.75 |
| **3** | 16±0.82 | 30±0.22 | 20±0.24 | 7±0.25 | 36±0.33 | 21±1.00 | 28±0.51 | 7±0.14 |
| **4** | 18±0.37 | 32±0.72 | 26±0.24 | 30±1.08 | 20±0.66 | 21±0.22 | 32±0.28 | 40±0.49 |
| Penicillin | 18±0.14 | 12±0.12 | 18±0.14 | 16±0.16 | 10±0.12 | 13±0.12 | 14±0.13 | 13±0.10 |
| Ampicillin | 12±0.10 | 13±0.12 | 14±0.17 | 14±0.11 | 12±0.08 | 14±0.09 | 12±0.11 | 16±0.13 |
| Vancomycine | 22±0.22 | 19±0.17 | 22±0.22 | 21±0.19 | 26±0.45 | 18±0.16 | 18±0.20 | 13±0.17 |
| Tetracycline | 28±0.54 | 25±0.35 | 30±0.22 | 24±0.31 | 28±0.26 | 23±0.22 | 25±0.17 | 26±0.21 |
| DMSO | Na | Na | Na | Na | Na | Na | Na | Na |

Experiment was performed in triplicate and expressed as mean ± SD.

Table 6. Comparison of the average inhibition zone resulted from the synthesized compounds with the other metal-ylide complexes as reported in literature.

| Microorganism | Inhibition zone (mm) | | |
|---|---|---|---|
| | *B. cereus* | *S. aureus* | *E. coli* |
| Hg(II) complex of sulfurylide (this work) | 28.75 | 21.75 | 16 |
| Hg(II) complex of phosphoniumylide [36] | 44 | 30 | - |
| Hg(II) complex of sulfurylide [37] | 19.66 | 24 | 20.33 |
| Pd(II) complex of phosphine ylide [38] | - | 15.25 | - |
| Cu(I) complex of phosphine ylide [39] | 12.25 | 17.25 | 14.75 |

Table 7. X-ray diffraction (XRD) data.

| Entry | Complexes | 2θ | Peak width (degree) (FWHM) |
|---|---|---|---|
| **1** | 1 | 12.67 | 0.196 |
| | 2 | 11.97 | 0.147 |
| | 3 | 11.89 | 0.147 |
| **2** | 1 | 12.94 | 0.147 |
| | 2 | 12.3 | 0.196 |
| | 3 | 13.82 | 0.344 |
| **3** | 1 | 26.46 | 0.246 |
| | 2 | 28.69 | 0.196 |
| | 3 | 25.91 | 0.295 |
| **4** | 1 | 28.12 | 0.246 |
| | 2 | 28.69 | 0.196 |
| | 3 | 28.42 | 0.196 |
| **5** | 1 | 31.55 | 0.344 |
| | 2 | 32.01 | 0.246 |
| | 3 | 31.48 | 0.196 |
| **6** | 1 | 37.30 | 0.393 |
| | 2 | 37.01 | 0.196 |
| | 3 | 37.04 | 0.344 |
| **7** | 1 | 39.29 | 0.295 |
| | 2 | 39.67 | 0.196 |
| | 3 | 39.42 | 0.246 |
| **8** | 1 | 47.29 | 0.196 |
| | 2 | 46.40 | 0.246 |
| | 3 | 46.34 | 0.246 |

## Graphical abstract